Published in Optics Letters 26, issue 12, 887-889, 2001
which should be used for any reference to this wor

Photoacoustic spectroscopy with quantum cascade distributed-feedback lasers

Daniel Hofstetter, Mattias Beck, and Jérôme Faist
Institute of Physics, University of Neuchâtel, 1 A.-L. Breguet, CH-2000 Neuchâtel, Switzerland

Markus Nägele and Markus W. Sigrist
Institute of Quantum Electronics, Swiss Federal Institute of Technology, CH-8093 Zürich, Switzerland

We present photoacoustic (PA) spectroscopy measurements of carbon dioxide, methanol, and ammonia. The light source for the excitation was a single-mode quantum cascade distributed-feedback laser, which was operated in pulsed mode at moderate duty cycle and slightly below room temperature. Temperature tuning resulted in a typical wavelength range of 3 cm^{-1} at a linewidth of 0.2 cm^{-1}. The setup was based on a Herriott multipass arrangement around the PA cell; the cell was equipped with a radial 16-microphone array to increase sensitivity. Despite the relatively small average laser power, the ammonia detection limit was 300 parts in 10^9 by volume.

OCIS codes: 140.0140, 140.3490, 140.5960, 140.3070, 300.6430.

Single-mode quantum cascade (QC) lasers have become attractive light sources for mid-infrared absorption spectroscopy.[1–3] They have already been used in experimental configurations for photoacoustic (PA) spectroscopy[4] and for single-pass or multiple-pass absorption spectroscopy. For PA spectroscopy, however, these lasers have been operated at cryogenic temperatures, which require a quite advanced experimental setup.[4] The cryogenic operating conditions were necessary because room-temperature performance did not result in sufficiently low detection limits for PA spectroscopy. Recently, high performance distributed-feedback (DFB) QC lasers, whose room-temperature average power is sufficient for PA spectroscopy, were developed.[1,5] Until now, most PA spectroscopy experiments were made with CO or CO_2 lasers, which emit infrared radiation near 5 and 10 μm, respectively.[6,7] However, finding the overlap between the emission spectrum of these gas lasers and the absorption spectrum of the investigated gases can be problematic. In such a case, the use of quasi-continuous high-pressure CO_2 lasers offers a possible but sophisticated solution.[8] Another possible solution is the use of a light source based on difference-frequency generation between a pump and a signal laser beam in a nonlinear optical medium.[9] The preferred choice, however, is QC DFB lasers operated at or near room temperature. One can tune their emission wavelengths continuously over nearly 1% by simply changing the device temperature. If both design and operating conditions are carefully chosen, the emission peak can be swept across the absorption line of a particular gas.

The QC lasers used in the research described here are single-mode DFB lasers with surface gratings and lateral current injection. Details of their fabrication and main emission characteristics are discussed elsewhere.[1] But, inasmuch as the linewidth of a pulsed laser is a critical parameter, we first present some measurements of the linewidth dependence on electrical pulse length and device temperature. The laser linewidth was measured with either a grating spectrometer for low-resolution ($\Delta k > 0.16$ cm^{-1}) or a specifically designed Michelson interferometer for the high-resolution experiments. For both spectral measurements, the laser was placed into a Peltier-cooled aluminum box held at a constant temperature of $-30\,^{\circ}C$ and driven at 2.4 A ($I = 1.25 \times I_{th}$). For a duty cycle of 1.5% and a 40-ns pulse length, we found an average power level of 2 mW. A constant pulse repetition rate of 667 MHz and a variable pulse length of 3–80 ns was used. The filled circles in Fig. 1 show the full width at half-maximum of the linewidth as a function of pulse length. For pulses longer than 20 ns, we found almost linearly increasing linewidths of 0.18 cm^{-1} at 20 ns and of 0.55 cm^{-1} at 80 ns. For shorter pulses, the grating spectrometer resolution set the limit at $\sim$0.16 cm^{-1}.

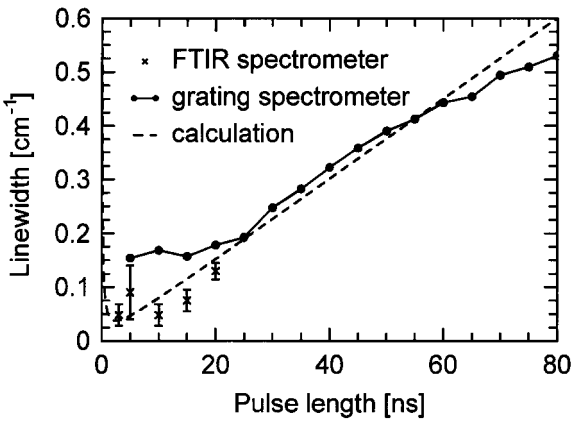

Fig. 1. Linewidth versus electrical pulse length for a QC DFB laser emitting at 10.4 μm. For the grating spectrometer data, there is a linewidth saturation at 0.16 cm^{-1} for pulse lengths below 20 ns. FTIR, Fourier-transform infrared spectrometer.

A more accurate determination of the linewidth can be achieved with a Fourier-transform infrared spectrometer with a sufficiently large displacement (i.e., 50 cm) of the movable mirror. One mirror was mounted onto an optical rail, and the other one was held upon a stepper-motor-driven linear stage. For several given positions of the first mirror on the optical rail, we measured the interference fringe contrast by tuning the movable mirror across 10 interference fringes. In Fig. 2 we thus show fringe contrast versus mirror displacement of the same laser as in Fig. 1 for four pulse lengths. In the inset, the corresponding spectra are presented. As shown by the crosses in Fig. 1, a linewidth minimum of 0.048 cm^{-1} at both 3 and 10 ns is observed, whereas slightly larger linewidths are seen when we go to 5 and 15 ns. In simple terms, the Fourier-transform limit sets a lower boundary for the linewidth of a QC-DFB lasers. Since heating dominates the linewidth for long pulses, one can write $\Delta v = C_1/t + C_2 t$. We obtained the constant $C_1 = 0.0466$ ns/cm by calculating the linewidths of transform-limited rectangular pulses, whereas C_2 was fitted to the experimental data. We attribute the deviation from the theory in Fig. 1 to three major causes. First, the gain profile created by the DFB grating will selectively amplify the wavelength corresponding to the peak of the gain curve. One can show, however, that for short pulses ($\tau \approx 3$ ns) the selection process does not have time to fully develop, thereby limiting the linewidth to $\Delta\nu \sim 0.1$ cm^{-1}. Second, we could not control the shape of the electrical pulse with high accuracy. In fact, a measurement of the optical pulse shape suggested that electrical ringing occurred, especially at 5 ns, and this resulted in a much larger error bar. Third, a Fourier-transform-limited linewidth can be seen only if the laser is operated near the gain maximum, where the linewidth enhancement factor α is close to zero. Depending on the detuning between the Bragg peak and the gain peak, the α factor can become as large as 0.5. Based on this effect, Paiella *et al.* recently demonstrated the operation of a QC laser in the mode-locked regime.[10]

Based on these results, we decided to work with pulse widths of 25 ns and a duty cycle of 3–4% for both lasers used in the following measurements. The PA cell used for these experiments was a 12-cm-long cylindrical chamber ($\varnothing = 6$ cm) with a 6-cm-long buffer volume ($\varnothing = 12$ cm) on each side. The laser entered and left the cell through two ZnSe Brewster windows. This whole setup was embedded between two spherical concave mirrors, which allowed for 36 passes of the light through the PA cell.[11] With an overall length of 70 cm and the number of passes, we ended up with a total optical path length of 24 m (15 m inside the PA cell). Because of the limited transmission per pass (96.1%), this path length resulted in a power enhancement factor of 19 (instead of 36 for 100% transmission). In the center of the PA cell, a radial microphone array with 16 microphones increased the signal-to-noise ratio (SNR) of the setup by a factor of 4. By chopping the beam mechanically at the first longitudinal resonance frequency of the cell ($f = 1250$ Hz), we gained another factor of 70 (i.e., the Q factor of the resonance) in the strength of the PA signal.[12] As a result of these three measures, we increased the PA signal by a factor of 64,000 compared with that of a nonresonant single-pass arrangement. The light of the QC laser was collected with a ZnSe lens ($f/1.0$), collimated, and then directed collinearly with a He–Ne laser beam for alignment purposes. Within the PA cell, the laser beam was left collimated; behind the cell, a pyroelectric detector recorded its power to normalize the PA signal. The setup is fully computer controlled, including control of the laser wavelength, the stabilization of the chopper frequency on the resonance frequency of the PA cell, and the data recording.

In Fig. 3 we present an absorption spectrum of pure CO_2 at atmospheric pressure in the wavelength range 981.5–984 cm^{-1}. Because of the changing average power of the laser, the SNR decreased from 20:1 at 984 cm^{-1} to 10:1 at 981.5 cm^{-1}. Good agreement between the experiment and the HITRAN data was seen. A minimum measurable absorption coefficient of $\alpha_{\min} = 2.2 \times 10^{-5}$ cm^{-1}, which corresponds to a minimal measurable line intensity of $S_{\min} = 2.5 \times 10^{-25}$ $cm^{-1}/(\text{molecule cm}^{-2})$, was determined.

Figure 4 shows a comparison between a FTIR absorption spectrum of methanol vapor (CH_3OH) at a

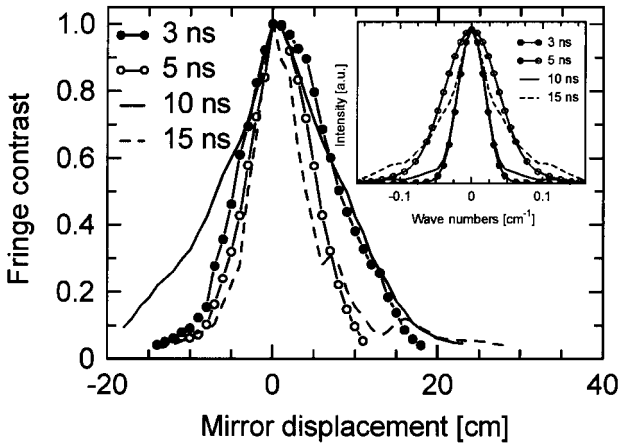

Fig. 2. Fringe contrast versus mirror position (interferogram) of a DFB QC laser for four pulse lengths. Inset, the corresponding spectra.

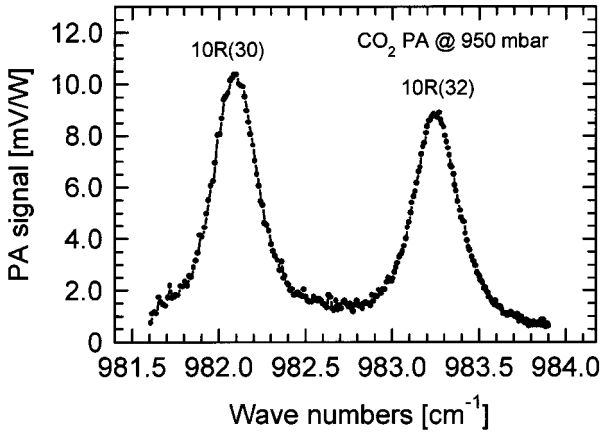

Fig. 3. PA absorption spectrum of CO_2 at 950 mbars (10 bars = 10^6 Pa) and at room temperature. The SNR decreases from 20 at 984 cm^{-1} to 10 at 981.5 cm^{-1}.

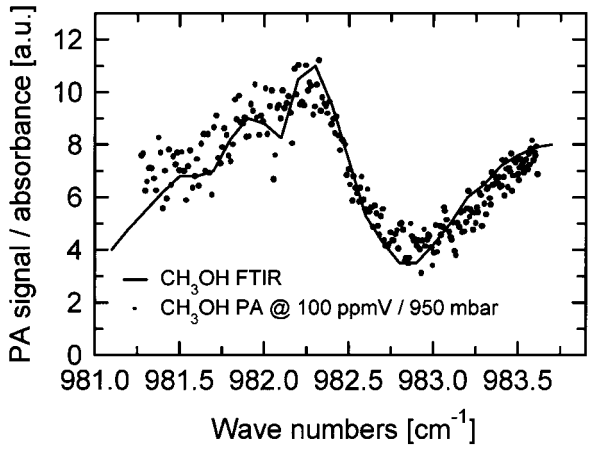

Fig. 4. Comparison of the absorption spectra of CH_3OH measured with a FTIR (550 ppmV buffered in synthetic air, 950 mbars, 300 K, 3-m path length) and measured by PA spectroscopy (100 ppmV buffered in synthetic air, 950 mbars, 300 K).

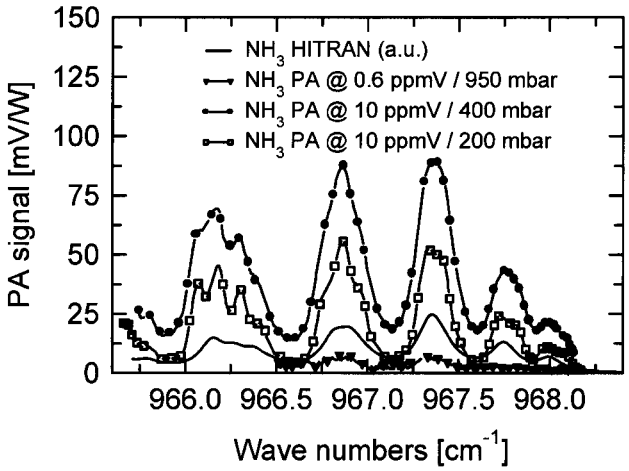

Fig. 5. Comparison of the absorption spectra of NH_3 based on the HITRAN database and based on PA spectroscopy [10 ppmV/400 mbars, 10 ppmV/200 mbars, 600 ppbV (0.6 ppmV)/950 mbars, all buffered in synthetic air at 300 K].

concentration of 500 parts in 10^6 by volume (ppmV) buffered in synthetic air (80% N_2 and 20% O_2) and a measurement by PA spectroscopy. The concentration for the PA experiment was 100 ppmV buffered in synthetic air at 950 mbars and for room temperature. The PA spectrum shows good agreement with the FTIR spectrum. However, because the QC wavelength could not be tuned to the strongest methanol absorption line at 1033 cm^{-1}, a rather large scattering of the PA data points is observed for a single measurement, i.e., without data averaging. Owing to the existence of higher laser powers at lower temperatures and larger wave numbers, the SNR of the measurement is much better for 983.5 cm^{-1} (SNR = 5) than for 981 cm^{-1} (SNR = 2.5). Based on an average SNR of 3, we estimate detection limits of 60 ppmV for this spectral position and of 5 ppmV for 1033 cm^{-1}.

In Fig. 5 several absorption spectra of ammonia diluted in synthetic air in the wavelength range 965–968 cm^{-1} are presented. Measurements at atmospheric pressure resulted in a relatively noisy spectrum. This result is presumably due to coupling of acoustic noise into the cell. For 400 mbars, the best SNR was achieved; at this pressure and concentration, the laser linewidth equals approximately that of the ammonia absorption features. We observed at lower pressure the convolution of the laser line shape with the absorption spectrum owing to the smaller pressure broadening of the ammonia lines. Because the microphone's responsivity decreases with lower pressure, the PA signal decreased as well; and this resulted again in a smaller SNR of the measurement. A value of 300 parts in 10^9 by volume (ppbV) at 400 mbars was identified as the detection limit for this particular configuration (with a SNR of 3). Good agreement with HITRAN data was achieved.

In conclusion, the use of a multiple-pass PA cell with a highly sensitive microphone array permitted the detection of ammonia concentrations as low as 300 ppbV (SNR of 3). This limit is expected to decrease even further when DFB QC lasers with higher output powers are used.[1]

The authors gratefully acknowledge the help of Jérôme Aubry and Thierry Aellen, who performed linewidth measurements. This study has been financially supported by the Swiss Priority Program Optique II, the Swiss National Science Foundation, and the Science Foundation of the European Community under the contract SUPERSMILE. D. Hofstetter's e-mail address is daniel.hofstetter@unine.ch.

References

1. D. Hofstetter, M. Beck, T. Aellen, and J. Faist, Appl. Phys. Lett. **78,** 396 (2001).
2. C. Gmachl, F. Capasso, J. Faist, A. L. Hutchinson, A. Tredicucci, D. L. Sivco, J. N. Baillargeon, S. N. G. Chu, and A. Y. Cho, Appl. Phys. Lett. **72,** 1430 (1998).
3. W. Schrenk, N. Finger, S. Gianordoli, L. Hvozdara, G. Strasser, and E. Gornik, Appl. Phys. Lett. **76,** 253 (1999).
4. B. A. Paldus, T. G. Spence, R. N. Zare, J. Oomens, F. J. M. Harren, D. H. Parker, C. Gmachl, F. Capasso, D. L. Sivco, J. N. Baillargeon, A. L. Hutchinson, and A. Y. Cho, Opt. Lett. **24,** 178 (1999).
5. R. Köhler, C. Gmachl, A. Tredicucci, F. Capasso, D. L. Sivco, S. N. G. Chu, and A. Y. Cho, Appl. Phys. Lett. **76,** 1092 (2000).
6. A. Olafsson, M. Hammerich, J. Bülow, and J. Henningsen, Appl. Phys. B **49,** 91 (1989).
7. S. Bernegger and M. W. Sigrist, Infrared Phys. **30,** 375 (1990).
8. P. Repond and M. W. Sigrist, IEEE J. Quantum Electron. **32,** 1549 (1996).
9. D. Richter, D. G. Lancaster, R. F. Curl, W. Neu, and F. K. Tittel, Appl. Phys. B **67,** 347 (1998).
10. R. Paiella, F. Capasso, C. Gmachl, D. L. Sivco, J. N. Baillargeon, A. L. Hutchinson, A. Y. Cho, and H. C. Liu, Science **290,** 1739 (2000).
11. D. Herriott, H. Kogelnik, and R. Kompner, Appl. Opt. **3,** 523 (1964).
12. A. Karbach and P. Hess, J. Chem. Phys. **84,** 2945 (1986).